

## Binary liquid phase separation and critical phenomena in a protein/water solution

(coacervation/coexistence curve/crystallization/lens proteins/phase transitions)

JOHN A. THOMSON\*, PETER SCHURTENBERGER, GEORGE M. THURSTON, AND GEORGE B. BENEDEK

Department of Physics and Center for Materials Science and Engineering, Massachusetts Institute of Technology, Cambridge, MA 02139

Contributed by George B. Benedek, April 14, 1987

**ABSTRACT** We have investigated the phase diagram of aqueous solutions of the bovine lens protein  $\gamma_{II}$ -crystallin. For temperatures  $T < T_c = 278.5$  K, we find that these solutions exhibit a reversible coexistence between two isotropic liquid phases differing in protein concentration. The dilute and concentrated branches of the coexistence curve were characterized, consistently, both by measurements of the two coexisting concentrations,  $c(T)$ , and by measuring the cloud temperatures for various initial concentrations. We estimate that the critical concentration,  $c_c$ , is 244 mg of protein per ml solution. The coexistence curve is well represented by  $|(c - c_c)/c_c| = 5.2\sqrt{(T_c - T)/T_c}$ . Using the temperature dependence of the scattered light intensity along isochores parallel to the critical isochore, we estimated the location of the spinodal line and found it to have the form  $|(c - c_c)/c_c| = 3.0\sqrt{(T_c - T)/T_c}$ . The ratio of the widths of the coexistence curve and the spinodal line, (5.2/3.0), is close to the mean-field value  $\sqrt{3}$ . We have also observed the growth of large crystals of  $\gamma_{II}$ -crystallin in some of these aqueous solutions and have made preliminary observations as to the factors that promote or delay the onset of crystallization. These findings suggest that selected protein/water systems can serve as excellent model systems for the study of phase transitions and critical phenomena.

Phase transitions and critical phenomena continue to be the subject of intensive experimental and theoretical investigation. In this context, systems consisting primarily of well-characterized proteins and water can serve as particularly valuable objects of study. Early experimental studies of phase equilibria in protein/water solutions were limited by inadequate purification and separation methods. In addition, theoretical progress was inhibited by an imprecise physicochemical understanding of protein structure. However, amino acid sequences and three-dimensional structures within crystalline states have been determined for a large number of proteins. Moreover, a wide variety of experimental techniques have provided much information about charge, hydration, and conformation of proteins in aqueous solution (1–3). With this information, the stage is set for a more quantitative experimental and theoretical examination of how the location and shape of aqueous phase boundaries might vary with a protein's precise molecular features, and with protein concentration, temperature, pressure, ionic environment, and other solvent characteristics.

The importance of studies of phase transitions in protein/water solutions derives also from their physiological relevance to the supramolecular organization of normal tissues and to certain pathological states. For example, such phase transitions play an important role in the deformation of the erythrocyte in sickle-cell disease (4) and in the cryoprecipitation of immunoglobulins in cryoglobulinemia and rheuma-

toid arthritis (5, 6). Perhaps the most striking example is the involvement of liquid–liquid phase separation in the opacification of the ocular lens fiber cell cytoplasm in certain forms of mammalian cataracts (7–11). Our work has indicated (12, 13) that the phase separation of one class of lens proteins, the  $\gamma$ -crystallins, may be the dominant mechanism responsible for the loss of transparency in such cataracts.

Liquid–liquid phase separation in protein solutions has been studied by a number of investigators. Bungenberg de Jong (14) studied liquid–liquid phase separation extensively in a variety of colloidal systems, including aqueous protein solutions. He induced phase separation by the addition of simple electrolytes, polyelectrolytes, and organic solvents miscible with water. He regarded such phase separations as a subset of a broader phenomenon, which he termed coacervation. Dervichian (15) also studied liquid–liquid phase separation in aqueous protein solutions and constructed phase diagrams with which to represent his findings. Similar investigations continue to be reported. Most of these studies have been largely exploratory in character, with an emphasis on application to protein separation methods (16, 17) and to microencapsulation (18, 19) and on the qualitative classification of the effects of additives on the phase separations (14, 15). Relatively little work has been devoted to the study of phase separation in protein water solutions as a model system to investigate the basic statistical mechanics of critical phenomena and to examine the fundamental interaction energies acting between the constituent protein molecules. One notable exception has been the work of Ishimoto and Tanaka (20) and Tanaka, Nishio, and Sun (21), who studied phase separation in aqueous lysozyme solutions using light scattering methods.

In this paper, we report our development of an experimental system that we believe will prove quite useful for the study of liquid–liquid phase separation and crystallization in protein solutions. The system comprises aqueous solutions of the bovine lens protein  $\gamma_{II}$ -crystallin. The  $\gamma$ -crystallins are a closely related, structurally homologous, family of monomeric proteins that appear to be expressed in all mammalian lenses (22, 23).  $\gamma$ -Crystallins appear to be structural proteins, in the sense that they have no apparent enzymic, ligand-binding, or other specific biological functions. They are small ( $M_r \approx 20,000$ ), compact, globular proteins, with isoelectric points close to neutrality (pH 7–8). Bovine  $\gamma_{II}$ -crystallin is the only  $\gamma$ -crystallin for which both the amino acid sequence (24–26) and an x-ray crystal structure (25, 27) have been determined. It has an extremely symmetrical conformation, in which two similar domains pack tightly against one

Abbreviations:  $T$ , temperature;  $T_c$ , critical temperature for phase separation;  $T_{sp}$ , spinodal temperature;  $T(\text{cloud})$ , temperature for onset of phase separation;  $T(\text{clarify})$ , minimum temperature at which the solution clarified;  $c$ , concentration in mg/ml;  $c_c$ , critical concentration for phase separation;  $I(\theta)$ , intensity of light scattered at scattering angle  $\theta$ .

\*To whom reprint requests should be addressed.

The publication costs of this article were defrayed in part by page charge payment. This article must therefore be hereby marked "advertisement" in accordance with 18 U.S.C. §1734 solely to indicate this fact.

another, mainly through hydrophobic interactions and hydrogen bonding. Each domain is itself internally symmetrical, and stabilized by a hydrophobic core and a high degree of surface ion pairing (25, 27, 28). It has been proposed that these are the features primarily responsible for the remarkable thermal and chemical stability of  $\gamma_{II}$ -crystallin (23), which has been demonstrated in many studies (see refs. 23 and 27).

## MATERIALS AND METHODS

Bovine  $\gamma_{II}$ -crystallin was prepared as follows. Lenses from 1- to 2-week-old calves were homogenized at 20°C in five volumes of 100 mM sodium phosphate buffer (adjusted to pH 7.00 with HCl to give a final chloride ion concentration of 2.3 mM), and the total monomeric crystallins were isolated from the centrifuged extract by size-exclusion chromatography, on a column of Sephadex G-75 (5.0 × 110 cm) at 20°C. The mixture of monomeric crystallins was separated into fractions  $\gamma_I$ ,  $\beta_s$ ,  $\gamma_{II}$ ,  $\gamma_{III}$ , and  $\gamma_{IV}$  by ion-exchange chromatography on Sulfopropyl (SP)-Sephadex C-50, using a variation of the method described by Bjork (29). The proteins ( $\approx 3$  g) were dialyzed exhaustively against 0.275 M sodium acetate buffer (pH 4.80) and applied to a column (2.5 × 35 cm), which had been equilibrated in the same buffer. The individual fractions were eluted from the column with a linear salt gradient of 0 to 0.4 M NaCl in 0.275 M sodium acetate (total volume, 2.2 liters). The pooled crude  $\gamma_{II}$ -crystallin fraction was reconcentrated by ultrafiltration (20°C, using an Amicon PM10 membrane) and dialyzed into 25 mM ethanolamine buffer (pH 9.50) for rechromatography on a column of diethylaminoethyl (DEAE)-cellulose, equilibrated in the same buffer. The remaining traces of contaminating polypeptides (mostly  $\beta_s$ - and  $\gamma_{III}$ -crystallins) were separated from the  $\gamma_{II}$ -crystallins by eluting the proteins from the DEAE-cellulose column with a linear salt gradient of 0 to 0.1 M NaCl in 25 mM ethanolamine (total volume, 1.8 liters). The final  $\gamma_{II}$ -crystallin fraction was demonstrated to be >99% pure by analytical isoelectric focusing, using gels containing 6 M urea, followed by densitometric scanning, as described (30).

After combining numerous individual  $\gamma_{II}$ -crystallin preparations, the protein was concentrated to  $\approx 150$  mg/ml by ultrafiltration (as described above). To obtain more concentrated solutions (>400 mg/ml), this material was dialyzed against 20% (wt/vol) polyethylene glycol 8000 until the volume of the protein solution was sufficiently reduced. Thereafter, all protein solutions were dialyzed exhaustively against 100 mM sodium phosphate buffer (pH 7.00;  $I = 0.24$ ) for all physical studies. Protein concentrations were determined by UV absorption spectroscopy, using a specific absorbance coefficient ( $A_{280}^{0.1\% \cdot 1 \text{ cm}}$ ) of 2.4 (J.A.T., unpublished results), and all sample dilutions were made using the final dialysate. Solutions that were not used immediately were stored at 4°C.

The intensity of the light scattered from the protein solutions was determined using an argon-ion laser [Spectra Physics model 164; wavelength 488 nm (Spectra Physics, Santa Clara, CA)] and a photomultiplier [EMI model 9863A (EMI, Hayes, Middlesex, U.K.)] mounted on a rotary table. Approximately 200  $\mu$ l of solution were placed in cylindrical scattering tubes having an inner diameter of 4 mm. The temperature of the tubes was controlled to within  $\pm 0.1^\circ\text{C}$ . Intensity measurements were performed at a scattering angle of  $\pi/2$ . The spectrometer permits visual observations of the transmitted beam and microscopic (up to 100 $\times$ ) visual observation of the scattering volume.

## RESULTS AND DISCUSSION

Two methods were used to determine the coexistence curve for phase separation, which specifies the two concentrations of the liquid phases coexisting in equilibrium at a given temperature (31). In the first, solutions of known concentration were placed in the light-scattering spectrometer, the temperature was initially fixed to be well above the coexistence curve, and the temperature was then slowly lowered. The onset of phase separation into two phases, at temperature  $T(\text{cloud})$ , was marked by the disappearance of the transmitted beam due to extensive multiple scattering of the incident beam. There was a concomitant clouding of the solution that could be easily observed visually. If the temperature was allowed to remain at or below this clouding temperature, the solution would, in most cases (see below), form two clear phases, which were separated by a sharp meniscus. However, for the method being described, this separation was not permitted to take place. Rather, the temperature was raised slightly as soon as the onset of clouding was observed, until the solution clarified, the transmitted beam reappeared, and the intensity of the scattered light returned to the appropriate value observed prior to clouding. We denote by  $T(\text{clarify})$  the minimum such temperature at which the solution clarified. The averages of the  $T(\text{cloud})$  and  $T(\text{clarify})$  so determined are plotted as filled circles in Fig. 1. The error bars show representative values of the quantity  $[T(\text{clarify}) - T(\text{cloud})]$ .

In the second method for determining the coexistence curve, solutions at an initial temperature well above the coexistence curve were rapidly quenched to temperatures below their cloud points, by immersing them in a circulating water bath [Neslab model RTE-5DD (Neslab, Portsmouth, NH)]. Phase separation commenced, and the solutions were allowed to undergo a macroscopic, gravity-driven separation into the two coexisting phases. At temperatures above 0°C, both phases became quite transparent within  $\approx 2$  hr and were

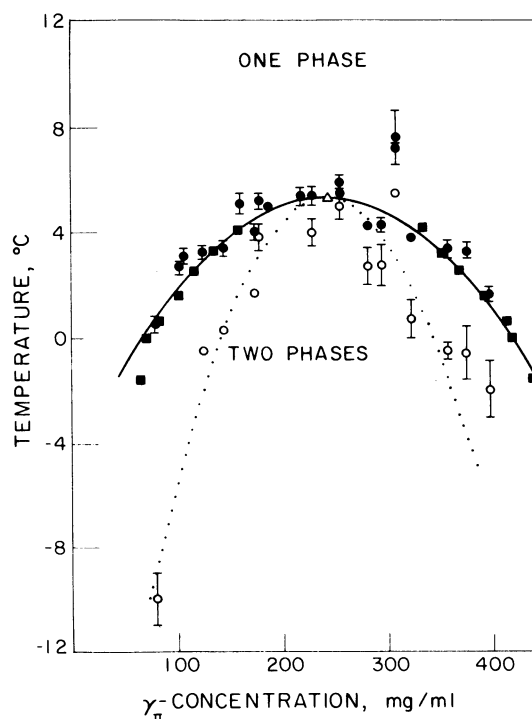


FIG. 1. Coexistence curve and spinodal line for the aqueous  $\gamma_{II}$ -crystallin system (pH = 7.0,  $I = 0.24$ ). ●, Cloud-point determinations; ■, concentration measurements of macroscopically separated phases; △, critical point; ○, spinodal temperature estimates; solid line, Eq. 1; dotted line, Eq. 2.

separated by a sharp meniscus. Below 0°C, repeated immersions in the bath, alternating with gentle centrifugation at approximately the same temperature as the bath temperature, were necessary to allow small bubbles of the less-dense, less-concentrated phase to escape from the highly viscous, more-concentrated phase. Eventually the two phases became quite transparent at the quench temperature and were separated by a sharp meniscus. The concentrations of the two phases were then determined by UV absorption spectroscopy in the manner described above, using small aliquots from each phase. Each quench thus resulted in the determination of a pair of concentrations on the coexistence curve, at the quench temperature. Seven such pairs of concentrations are plotted as the filled squares in Fig. 1.

Fig. 1 clearly shows that these two independently determined sets of concentrations and temperatures on the coexistence curve (one set resulting from the clouding and clarification temperatures and the other set determined using quench-induced macroscopic phase separations) are in good agreement.

A mean-field theoretical treatment of such a phase separation would predict that the shape of the coexistence curve is parabolic in the vicinity of the critical point (32). We have, therefore, performed a fit of the coexistence curve, as it was determined by the quench method, to the expression

$$|(c - c_c)/c_c| = A[(T_c - T)/T_c]^{1/2}, \quad [1]$$

where  $c$  is the concentration of either phase in mg/ml,  $c_c$  is the critical concentration,  $T_c$  is the critical temperature in K, and  $A$  is a dimensionless quantity that characterizes the width of the coexistence curve. We find that our data are represented within experimental error by the values  $c_c = 244 \pm 10$  mg/ml,  $T_c = 278.5 \pm 0.2$  K, and  $A = 5.2 \pm 0.1$ . The critical point and coexistence curve corresponding to these parameters and to Eq. 1 are shown by the open triangle and by the solid curve, respectively, in Fig. 1.

While observing the coexistence curve by the first method described above, the intensity  $I(\pi/2)$  of the light scattered at a scattering angle of  $\theta = \pi/2$  was also measured as a function of temperature,  $T$ . As the temperature of the sample was lowered, so that the coexistence curve was approached, this intensity increased dramatically. We used the measured temperature dependence of  $I(\pi/2)$  to estimate the location of the spinodal line that is associated with this liquid-liquid phase separation. The mathematical condition for this boundary is the vanishing of the second derivative, with respect to concentration, of the molar Gibbs free energy of such a mixture (31). In this connection, the limit, as  $\theta$  approaches 0, of the intensity  $I(\theta)$  of the light scattered by a macroscopically homogeneous binary liquid mixture, which is in thermodynamic equilibrium, is inversely proportional to this same second derivative of the Gibbs free energy (33). This implies that  $I(0)$  would diverge at the spinodal line, if the solution were to remain in a single phase on approaching this line. If the experimental observations were to conform to a mean-field theoretical treatment, this divergence would be described by  $I(\theta = 0, c) = A/[T - T_{sp}(c)]$ , where  $T_{sp}(c)$  is the spinodal temperature at concentration  $c$ . Indeed, for all concentrations studied, we were able to identify a substantial temperature range over which even  $I^{-1}(\pi/2)$  was found to vary linearly with the temperature. Since our solutions did not remain homogeneous in the relevant region of the phase diagram at temperatures below the cloud-point temperature, we estimated  $T_{sp}(c)$  from linear extrapolations of the measured values of  $I^{-1}(\pi/2, c)$  vs.  $T$  to temperatures below  $T(\text{cloud})$ , to find the temperatures at which the extrapolated lines intersect the axis  $I^{-1}(\pi/2) = 0$ . The resulting estimates of  $T_{sp}(c)$  are plotted as the open circles in Fig. 1. It is important to note that, notwithstanding some scatter in the

data presented in Fig. 1, the coexistence curve temperatures and the spinodal line temperatures become quite similar for concentrations in the vicinity of the maxima of both curves. Indeed, the spinodal line and the coexistence curve must converge at this maximum, which is the critical point, for a second-order phase transition such as a liquid-liquid phase separation (31). A fit of the estimated spinodal points to the expression

$$|(c - c_c)/c_c| = B[(T_c - T)/T_c]^{1/2} \quad [2]$$

was also performed. With use of the values of  $c_c$  and  $T_c$  already determined, we find that the value  $B = 3.0$  gives a good representation of the experimental points. The corresponding spinodal line is shown by the dotted line in Fig. 1. In the context of a mean-field theory, the ratio of widths of the coexistence curve and the spinodal line,  $[A/B]$ , should be close to  $\sqrt{3}$  in the vicinity of the critical point (34). The experimentally determined ratio is  $[5.2/3.0] \approx 1.7$ , which is equal to  $\sqrt{3}$  within the experimental uncertainty.

For concentrations well away from the critical concentration  $c_c = 244$  mg/ml, we found that  $I^{-1}(\pi/2)$  was quite linear as a function of temperature at all of the investigated temperatures above  $T(\text{cloud})$ , allowing a relatively accurate extrapolation to  $I^{-1}(\pi/2) = 0$ . However, at concentrations quite close to the critical concentration, while  $I^{-1}(\pi/2)$  was linear over the high temperature part of the range of temperatures investigated, it also showed some nonlinearity at temperatures close to  $T(\text{cloud})$ . This nonlinearity introduces uncertainty into the choice of the line we used to estimate  $T_{sp}$ . Such a nonlinear dependence is shown by the values of  $I^{-1}(\pi/2)$  for  $c = 256$  mg/ml, which are plotted in Fig. 2 as the solid squares. The solid line in Fig. 2 shows the linear extrapolation used to estimate  $T_{sp}(256 \text{ mg/ml})$ . Possible

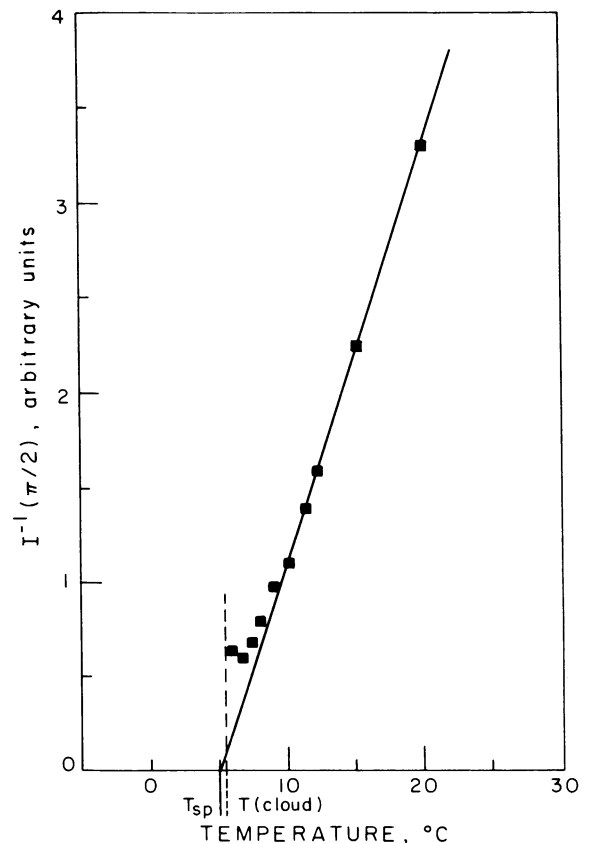


FIG. 2. Inverse scattered intensity at scattering angle  $\pi/2$  as a function of temperature, for  $c = 256$  mg/ml.

sources of this nonlinearity include (i) an increase in the spatial correlation range  $\xi$  of the concentration fluctuations in the solution in the vicinity of the critical point, (ii) increased multiple scattering of light, and (iii) deviations from mean-field critical exponents. These considerations could also affect the observed  $I^{-1}(\pi/2)$  well away from the critical concentration. Thus our determinations of the location and shape of the spinodal line are less certain than our determinations of the coexistence curve.

In addition to liquid-liquid phase separation, we occasionally observed the spontaneous growth of isomorphous crystals of  $\gamma_{II}$ -crystallin and/or the formation of a macroscopically amorphous solid phase. We have gained experience as to factors that prevent or promote the formation and growth of these solid phases. In particular, we found that meticulous attention to cleanliness and to filtration of solutions and the cleanliness of glassware, as well as the routine degassing of buffers and subsequent saturation with nitrogen, tended to completely inhibit the formation of the amorphous solid phase—presumably by preventing protein oxidation and denaturation. These procedures also significantly retarded the nucleation of isomorphous crystals. It should be stressed that the determinations of the coexistence curve and spinodal line reported above were performed in solutions in which we did not observe growth of any solid phases in the scattering volume, at the 100 $\times$  magnification available on the light-scattering spectrometer used. We found that the presence of solid phases could quite easily affect the scattered intensity sufficiently to confound the methods described above for the estimation of the spinodal and cloud-point temperatures.

To determine the coexistence curve and the spinodal line, any crystals that had grown, due to storage of the solution at 4°C, were dissolved by gentle heating of the solution. Our experience with this procedure has given us some information about the composition of the liquid phase that would be in equilibrium with the solid crystals at a given temperature. These composition-temperature pairs ( $c, T$ ) comprise a boundary called the liquidus (34). We have found two approximate positions on the liquidus. First, we found that at  $c = 295$  mg/ml, crystals present would completely dissolve if the temperature was raised to between 35°C and 39°C. Second, if crystal growth was permitted to proceed in a solution, both macroscopic liquid-liquid phase separation and crystallization could be observed at temperatures below the coexistence boundary. However, after a period of weeks of storage at 4°C, the crystal(s) present in the individual solutions had grown to incorporate enough material so that the denser of the two liquid phases was no longer present. This implies that the liquidus has a lower concentration than that corresponding to the dilute branch of the coexistence curve at 4°C. From these two approximate locations of the liquidus boundary in the  $\gamma_{II}$ -crystallin and water system, we can conclude that this boundary satisfies  $(dT/dc) > 0$ . If the temperature is raised above this boundary, for a fixed overall solution composition, the crystals will completely dissolve. Likewise, they will dissolve if the solutions are diluted, at fixed temperature, to overall concentrations smaller than those of the boundary. While further experiments are needed to locate the liquidus more precisely, the information just presented about its location indicates that at least part of the liquid-liquid coexistence curve presented in Fig. 1 is actually metastable with respect to crystal growth.

The phenomena of crystal formation and growth has also been reported (20, 35) for phase-separating aqueous solutions of lysozyme and water. This has given rise to controversy in the literature as to the interpretation of the phase boundaries that have been observed for this system. Ishimoto and Tanaka (20) reported a cloud-point curve and underlying spinodal curve in the lysozyme/water system that they interpreted as corresponding to a coexistence curve and

underlying spinodal for a second-order phase separation. They also reported the slow formation of crystals of lysozyme in their solutions but took precautions in the attempt to prevent this crystal growth from disturbing the interpretation of their light-scattering measurements. On the other hand, Phillies (35) has made observations of similar aqueous lysozyme solutions, in which he observed crystal formation and growth, but no phase separation that would correspond to that reported by Ishimoto and Tanaka (20). He suggested that the scattering observed by the latter workers might be attributable to the formation of small crystals in the solution.

In contrast to the reported observations about aqueous lysozyme systems, the present aqueous  $\gamma_{II}$ -crystallin system does exhibit macroscopic, reversible liquid-liquid phase separation, in which both the concentrated and the dilute phases are transparent. However, since the portion of the phase diagram that describes this phase separation is metastable with respect to equilibrium between a solid, crystalline phase and a single liquid phase, it was necessary to take the precautions described above to retard crystal formation and thereby to enable the clear observation of liquid-liquid separation. Also as described above, gentle centrifugation was necessary to effect a macroscopic phase separation, at the lower temperatures investigated. Similar procedures could prove to be of use in experimental investigations of the mentioned phase boundaries reported in aqueous lysozyme systems. It is interesting to note that the location of the crystallization boundary (liquidus) reported by Phillies (35) for lysozyme is at higher temperatures than the phase-separation boundary reported by Ishimoto and Tanaka (20). If both boundaries were to be verified, this situation would then be qualitatively similar to that which we have observed, and described above, for the case of  $\gamma_{II}$ -crystallin solutions.

The coexistence curve reported here (Fig. 1) differs from the opacification curve obtained by Siezen *et al.* (12) for bovine  $\gamma_{II}$ -crystallin. The opacification curve was obtained for concentrations up to 195 mg/ml (recalculated using  $A_{280}^{0.1\%, 1\text{cm}} = 2.4$ ), which is below the critical concentration we find,  $c_c = 244$  mg/ml. At corresponding values of  $\gamma_{II}$ -crystallin concentration, the opacification curve is displaced upward in temperature by 4–5°C from the curve of Fig. 1. The opacification curve determined by Siezen *et al.* (12) was obtained with use of a 50 mM sodium phosphate buffer (pH = 7.0,  $I = 0.11$ ) in contrast to the 100 mM sodium phosphate buffer (pH = 7.0,  $I = 0.24$ ) used in the present work. The 4 to 5°C temperature displacement is consistent with the ionic strength dependence of the coexistence curve (J.A.T., unpublished results). It should also be noted that the data presented by Siezen *et al.* (12) represent cloud-point measurements alone. On the other hand, our cloud-point measurements, which cover a much larger concentration range, were complemented by measurements of the equilibrium concentrations following macroscopic separation of the solution into two transparent liquid phases. It is important to keep in mind that we found that the equilibrium between the two liquid phases is metastable with respect to the formation of a solid phase coexisting with a liquid phase. In the course of our studies, we noted that factors that enhanced the formation rate of the solid phase could confound cloud-point measurements, due to increased light scattering from the solid phase. To minimize this effect, we adopted the procedure of centrifuging concentrated samples at moderately high temperatures (35–40°C) to melt or sediment the nucleation sites. Also as noted above, factors that would tend to retard protein oxidation also retarded the actual formation of the solid phase.

The experiments reported here demonstrate that aqueous  $\gamma_{II}$ -crystallin solutions undergo a second-order, liquid-liquid phase transition, analogous to the liquid-gas phase transition of a pure fluid. A similar analogy has already been described

by Prouty *et al.* (36) in their studies of the phase diagram of deoxyhemoglobin-S. Our measurements also revealed the approximate location of a solid-liquid phase boundary in the  $\gamma_{11}$ -crystallin and water system. Further studies of the equilibrium properties associated with the liquid phases, such as the osmotic pressure, the osmotic compressibility, the specific heat, and the correlation range, can establish the equation of state of such solutions. This in turn can aid in the formulation of a theoretical expression for the Gibbs free energy corresponding to these phases. Also a more detailed study of the location of the solid-liquid phase boundary can provide information on the Gibbs free energy associated with the solid phase. Once the Gibbs free energies of these phases are characterized, it will be of great importance to determine how the parameters entering therein change with solution conditions such as pH and ionic strength and with the amino acid sequence and three-dimensional structure of the individual proteins themselves. In this way it should be possible to relate the phase diagrams obtained experimentally to the fundamental molecular properties of the constituents of these systems.

This work was supported by the National Eye Institute of the National Institutes of Health (grants 5-RO1-EY05496-03 and 2-RO1-EY05127-03), by the National Science Foundation (grant 8408630-DMB), and by the Jesse B. Cox Charitable Trust.

1. Cantor, C. R. & Schimmel, P. R. (1980) *Biophysical Chemistry* (Freeman, San Francisco), Parts I, II and III.
2. Creighton, T. E. (1983) *Proteins* (Freeman, New York).
3. Schulz, G. E. & Schirmer, R. H. (1979) *Principles of Protein Structure* (Springer, New York).
4. Noguchi, C. T. & Schechter, A. N. (1985) *Annu. Rev. Biophys. Biophys. Chem.* **14**, 239-263.
5. Brandau, D. T., Trautman, P. A., Steadman, B. L., Lawson, E. Q. & Middaugh, C. R. (1986) *J. Biol. Chem.* **261**, 16385-16389.
6. Middaugh, C. R., Gerber-Jensen, B., Harvitz, A., Paluszek, A., Scheffel, C. & Litman, G. W. (1978) *Proc. Natl. Acad. Sci. USA* **75**, 3440-3444.
7. Tanaka, T. & Benedek, G. B. (1975) *Invest. Ophthalmol.* **14**, 449-456.
8. Ishimoto, C., Goalwin, P. W., Sun, S.-T., Nishio, I. & Tanaka, T. (1979) *Proc. Natl. Acad. Sci. USA* **76**, 4414-4419.
9. Clark, J. I., Giblin, F. J., Reddy, V. N. & Benedek, G. B. (1982) *Invest. Ophthalmol.* **22**, 186-190.
10. Benedek, G. B., Clark, J. I., Serrallach, E. N., Young, C. Y., Mengel, L., Sauke, T., Bagg, A. & Benedek, K. (1979) *Phil. Trans. R. Soc. London Ser. A* **293**, 329-340.
11. Clark, J. I. & Carper, D. (1987) *Proc. Natl. Acad. Sci. USA* **84**, 122-125.
12. Siezen, R. J., Fisch, M. R., Slingsby, C. & Benedek, G. B. (1985) *Proc. Natl. Acad. Sci. USA* **82**, 1701-1705.
13. Siezen, R. J. & Benedek, G. B. (1985) *Curr. Eye Res.* **4**, 1077-1085.
14. Bungenberg de Jong, H. G. (1949) in *Colloid Science*, ed. Kruyt, H. R. (Elsevier, Amsterdam), Vol. II, pp. 232-258.
15. Dervichian, D. G. (1954) *Discuss. Faraday Soc.* **18**, 231-239.
16. Veis, A. (1964) *The Macromolecular Chemistry of Gelatin* (Academic, New York).
17. Stainsby, G. (1977) in *The Science and Technology of Gelatin*, eds. Ward, A. G. & Courts, A. (Academic, London), pp. 109-136.
18. Clark, R. C. & Courts, A. (1977) in *The Science and Technology of Gelatin*, eds. Ward, A. G. & Courts, A. (Academic, London), pp. 209-247.
19. Wood, P. D. (1977) in *The Science and Technology of Gelatin*, eds. Ward, A. G. & Courts, A. (Academic, London), pp. 413-437.
20. Ishimoto, C. & Tanaka, T. (1977) *Phys. Rev. Lett.* **39**, 474-477.
21. Tanaka, T., Nishio, I. & Sun, S.-T. (1981) in *Scattering Techniques Applied to Supramolecular and Nonequilibrium Systems*, eds. Chen, S.-H., Chu, B. & Nossal, R. (Plenum, New York), pp. 703-724.
22. Schoenmakers, J. G. G., den Dunnen, J. T., Moorman, R. J. M., Jongblod, R., van Leen, R. W. & Lubsen, N. H. (1984) in *Human Cataract Formation*, CIBA Foundation Symposium, eds. Nujent, J. & Whelan, J. (Pitman, London), Vol. 106, pp. 208-218.
23. Summers, L., Slingsby, C., White, H., Narebor, M., Moss, D., Miller, L., Mahadevan, D., Lindley, P., Driessen, H., Blundell, T., den Dunnen, J., Moorman, R., van Leen, R. & Schoenmakers, J. (1984) in *Human Cataract Formation*, CIBA Foundation Symposium, eds. Nujent, J. & Whelan, J. (Pitman, London), Vol. 106, pp. 219-236.
24. Croft, L. R. (1972) *Biochem. J.* **128**, 961-970.
25. Wistow, G., Turnell, W., Summers, L., Slingsby, C., Moss, D., Miller, L., Lindley, P. & Blundell, T. (1983) *J. Mol. Biol.* **170**, 175-202.
26. Bhat, S. P. & Spector, A. (1984) *DNA* **3**, 287-295.
27. Blundell, T., Lindley, P., Miller, L., Moss, D., Slingsby, C., Tickle, I., Turnell, W. & Wistow, G. (1981) *Nature (London)* **289**, 771-777.
28. Poole, P. L. & Barlow, D. J. (1986) *Biopolymers* **25**, 317-335.
29. Bjork, I. (1964) *Exp. Eye Res.* **3**, 254-261.
30. Thomson, J. A. & Augusteyn, R. C. (1985) *Exp. Eye Res.* **40**, 393-410.
31. Guggenheim, E. A. (1967) *Thermodynamics* (North-Holland, New York).
32. Stanley, H. E. (1971) *Introduction to Phase Transitions and Critical Phenomena* (Oxford, New York).
33. McIntyre, D. & Gornick, F., eds. (1964) *Light Scattering from Dilute Polymer Solutions* (Gordon & Breach, New York).
34. Lupis, C. H. P. (1983) *Chemical Thermodynamics of Materials* (North-Holland, New York).
35. Phillies, G. D. J. (1985) *Phys. Rev. Lett.* **55**, 1341.
36. Prouty, M. S., Schechter, A. N. & Parsegian, V. A. (1985) *J. Mol. Biol.* **184**, 517-528.